The Finite Deformation of a Hollow Sphere subjected to Internal or External Pressure

AUTHOR(S):

YATOMI, Chikayoshi; KONDOH, Shinji

The Finite Deformation of a Hollow Sphere subjected to Internal or External Pressure

By

Chikayoshi YATOMI* and Shinji KONDOH*
(Received February 20, 1988)

Abstract

This paper is concerned with the deformation of a hollow sphere, within the theory of finite elastostatics for a particular homogeneous isotropic commpressible material, the so–called Blatz–Ko material. The body is subjected to uniform pressure, either internal or external. In the case of internal pressure, it is found that there is a maximum pressure beyond which there does not exist a solution. Under that pressure there exist two sets of solutions. In the case of external pressure, the location of the maximum value of the compressive hoop stress departs from the inner surface. There exists, howeverc a supremum of the location. If the hollow sphere is thinner than the supremum, the maximum value of the compressive hoop stress occurs at the outer surface.

1. Introduction

In this paper, we examine the deformation of a hollow sphere subjected to uniform internal or external pressure, within the theory of finite elastostatics for a particular homogeneous isotropic compressible material, the so–called Blatz–Ko material[1]. The constitutive equation of this material is relatively simple, and the system of partial differential equations governing the equilibrium equations ceases to be elliptic at sufficiently severe strain levels[2]. For such reasons, recently, Abeyaratne and Horgan[3] investigated the problem concerned with the plane strain deformation of a circular cavity in an infinite medium. In the case of a hollow sphere subjected to the internal pressure, it is found, interestingly, that the axisymmetric solutions are not unique. When the ratio of inner and outer radius b/a is given, there exists a certain maximum value of pressure P_{max} for the existence of the solutions. If the internal pressure P is smaller than P_{max}, there exist two sets of solutions for stress and deformation fields. Consequently, as P/μ (μ: the shear modulus) gets sufficiently small, we get another limit, which

---

*Department of Aeronautical Engineering

is diffrent from the result of the infinitesimal theory of elasticity. In the case of external pressure, the set of solutions is unique and is valid for an arbitrary large pressure. The hoop stress T_θ is compressive and its maximum value $|T_\theta|_{max}$ departs from the inner surface for a sufficiently large pressure. It is found, however, that the location of $|T_\theta|_{max}$ has its limitation, and if the hollow sphere is thinner than the limitation, $|T_\theta|_{max}$ ocuurs at the outer surface.

In both cases of internal or external pressure, we also examine the loss of ellipticity and the comparison with the infinitesimal theory.

2. Blatz-Ko material

Blatz-Ko material is a mathematical model of a particular homogeneous, isotropic, compressible elastic material. Within the finite elastic theory developed in 1960's, various experiments of rubberlike materials were exercised and their strain energy functions were proposed. Blatz-Ko material considered here is one of such materials composed of 47 per cent foamed polyurethane rubber, proposed by Blatz and Ko[1]. The elastic potential of this material is given by

$$W(I_1, I_2, I_3) = \frac{\mu}{2}\left(\frac{I_2}{J^2} + 2J - 5\right), \quad J = \sqrt{I_3}, \tag{1}$$

representing the strain energy per unit undeformed volume. Here, I_1, I_2, I_3 denote three invariants of the right Cauchy-Green deformation tensor $C = F^T F$ (F: deformation-gradient tensor). Using this elastic potential function, we find that in the state of plane-strain uni-axial tension (or compression) parallel to the X_1-axis, the relations between the principal stretches $\lambda_1, \lambda_2, \lambda_3$ and the Cauchy stress T_1, T_2, T_3 are

$$\lambda_3 = 1, \quad \lambda_2 = \lambda_1^{-1/3}, \quad T_2 = 0$$
$$T_1 = \mu(1 - \lambda_1^{-8/3}), \quad T_3 = \mu(1 - \lambda_1^{-2/3}).$$

As is apparent from these results, the Blatz-Ko material has a property that T_1 (λ_1) is a monotone increasing function and remains bounded in plane-strain uni-axial tension. Another property of this material is that the system of partial differential equations governing the equilibrium loses ellipticity at sufficiently severe strain levels.

3. Closed-form Solution

Using a similar method developed by Abeyaratne and Horgan[3], we obtain an exact closed-form solution to our problem describing finite deformation. Suppose that the region Ω_0 occupied by the undeformed body is a hollow sphere of inner radius a and outer radius b, and that the sphere is subjected to uniform internal or external pressure. The resulting (spherically symmetric) deformation is given by

$$R=R(r)>0, \quad \Theta=\theta, \quad \Phi=\phi, \quad on \ \Omega_0, \tag{2}$$

where we have used spherical polar coordinates (r, θ, ϕ) and (R, Θ, Φ) to describe the location of a particle is the underformed and deformed configurations, respectively. Unless explicitly stated oterwise, R (r) is assumed to be twice continuously differentiable on $r>a$.

The spherical components of the deformation gradient tensor $\boldsymbol{F}$ are found, using (2), to be

$$F_{rr}=\frac{\partial R(r)}{\partial r}, \quad F_{\theta\theta}=F_{\phi\phi}=\frac{R(r)}{r}, \tag{3}$$

with the remaining components of $\boldsymbol{F}$ being zero.

Since the Jacobian determinant $J=\det\boldsymbol{F}$ is required to be positive for the uniqueness of the local deformation,

$$\dot{R}(r)>0 \quad \text{for } a<r<b, \tag{4}$$

where the dot denoted differention with respect to its argument.

The principal stretches associated with the spherical deformation (2) are given by

$$\lambda_r=\dot{R}, \quad \lambda_\theta=\lambda_\phi=\frac{R}{r}, \tag{5}$$

so that the fundamental scalar invariants are expressed as

$$I_1=\dot{R}^2+\frac{2R^2}{r^2}, \quad I_2=\frac{R^4}{r^4}+\frac{2R^2\dot{R}^2}{r^2}, \quad I_3=\frac{\dot{R}^2R^4}{r^4}$$

$$J=\sqrt{I_3}=\frac{\dot{R}R^2}{r^2}. \tag{6}$$

From (6), the strain energy function (1) may be replaced by

$$W = \frac{\mu}{2}\left\{\frac{1}{R^2} + 2\frac{r^2}{R^2} + 2\frac{\dot{R}R^2}{r^2} - 5\right\}.$$ (7)

Since the Cauchy stress tensor $\boldsymbol{T}$ is given by

$$\boldsymbol{T} = \mu J^{-3}\left\{I_1\boldsymbol{B} - \boldsymbol{B}^2 + (J^3 - I_2)\boldsymbol{I}\right\}, \quad \boldsymbol{B} = \boldsymbol{FF}^T,$$

one finds from (3). (6) that

$$T_R = \mu\left\{1 - \frac{r^2}{\dot{R}^3 R^2}\right\}, \quad T_\theta = T_\phi = \mu\left\{1 - \frac{r^4}{\dot{R}R^4}\right\},$$ (8)

and otherwise zero.

In the absence of body forces, the equilibrium equations $div\boldsymbol{T} = \boldsymbol{0}$ reduce to the single equation

$$\frac{d}{dr}T_R + 2\frac{\dot{R}}{R}(T_R - T_\theta) = 0 \text{ for } a < r < b.$$ (9)

Introducing (8) to (9) yields the following nonlinear second-order ordinary differential equation for R (r).

$$3rR^3\ddot{R} - 2R^3\dot{R} + 2r^3\dot{R}^4 = 0 \quad \text{for } a < r < b.$$ (10)

This equation is reduced to a first-order equation on making the substitution

$$t = \frac{r\dot{R}}{R}\left(= \frac{\lambda_r}{\lambda_\theta}\right) > 0.$$ (11)

Equation (10) then yields

$$3r\frac{dt}{dr} + t(t-1)(2t^2 + 2t + 5) = 0 \quad \text{for } a < r < b.$$ (12)

Equation (12) may be readily integrated to yield

$$r^{15} = \frac{Ct^9h(t)}{(1-t)^5(2t^2 + 2t + 5)^2},$$ (13)

where C (> 0) is a constant of integration and we have set

$$h(t) = exp \left\{ 2\tan^{-1} \left(\frac{2t+1}{3} \right) \right\}. \tag{14}$$

on the other hand, eqns (11), (12) also geve

$$\frac{1}{R} \frac{dR}{dt} = \frac{3}{(1-t)(2t^2+2t+5)}, \tag{15}$$

which in turn yields

$$R^6 = \frac{D(2t^2+2t+5)h(t)}{(1-t)^2}, \tag{16}$$

Again, D (>0) is a constant of integration.
Eqns (13), (15), (16) provide a parametric exact solution to the differential equation (10).

4. Thecase of internal pressure

4.1. Solutions to the boundary conditions

When a hollow sphere is subjected to internal pressure, the range of the parameter t defined in (11) becomes $0 < t < 1$. (The detailed proof is omitted.) It is found from (12) that

$$\frac{dt}{dr} > 0, \ 0 < t < 1. \tag{17}$$

We find from (15), (17) that the deformed and undeformed radial coordinates (R, r) increase monotonically with t. Therefore the range of the parameter t becomes

$$(0<)t_a < t < t_b(<1), \tag{18}$$

where t_a, t_b are the values of t corresponding to $r=a, b$, which are to be determined from (13), i.e.,

$$a^{15} = \frac{Ct_a^9 h(t_a)}{(1-t_a)^5(2t_a^2+2t_a+5)^2} \tag{19}$$

$$b^{15} = \frac{Ct_b^9 h(t_b)}{(1-t_b)^5(2t_b^2+2t_b+5)^2}. \tag{20}$$

The components of the Cauchy stress T_R, T_θ (T_ϕ) may also be expressed in terms of t on using (8), (13), (16), (17). This leads to

$$T_R = \mu \left\{ 1 - \frac{(C^2/D^5)^{1/6}}{\sqrt{h(t)(2t^2+2t+5)^3}} \right\} \tag{21}$$

$$T_\theta = T_\phi = \mu \left\{ 1 - \frac{(C^2/D^5)^{1/6}}{\sqrt{h(t)(2t^2+2t+5)^3 t^{-4}}} \right\}. \tag{22}$$

Finally, we turn to the boundary conditions of the problem. Since the boundary conditions are

$$T_R = -P \quad at \quad r=a \tag{23}$$

$$T_R = 0 \quad at \quad r=b, \tag{24}$$

eqn (21) requires that

$$h(t_a)(2t_a^2+2t_a+5)^3(1+P/\mu)^2 = \left\{ \frac{C^2}{D^5} \right\}^{1/3} \tag{25}$$

$$h(t_b)(2t_b^2+2t_b+5)^3 = \left\{ \frac{C^2}{D^5} \right\}^{1/3}. \tag{26}$$

From (19), (20) and (25), (26) we obtain simultaneous equations concerning t_a and t_b, i. e.,

$$\frac{a^{15}(1-t_a)^5(2t_a^2+2t_a+5)^2}{t_a^9 h(t_a)} = \frac{b^{15}(1-t_b)^5(2t_a^2+2t_b+5)^2}{t_b^9 h(t_b)} \tag{27}$$

$$h(t_a)(2t_a^2+2t_a+5)^3(1+P/\mu)^2 = h(t_b)(2t_b^2+2t_b+5)^3. \tag{28}$$

When the ratio ot the inner and outer radius b/a and the internal pressure P are given, if (27), (28) can be solved fro t_a, t_b such that $0 < t_a < t_b < 1$, then (19), (25) provide the values of the constants $C, D (> 1)$, and eqns (13), (14) and (16) give the desired solution.

Here, we observe two auxiliary functions

$$H_1(t) = h(t)(2t^2+2t+5)^3 \tag{29}$$

$$H_2(t) + \frac{(1-t)^5(2t^2+2t+5)^2}{t^9 h(t)} \tag{30}$$

for $0 < t < 1$. It is easily shown that $\dot{H}_1(t) > 0$ for $0 < t < 0$, so $H_1(t)$ is a continuous monotone increasing function for $0 \le t \le 1$. Consequently, considering (18) and (28), P takes its maximum value $(P_{max})_\infty$ with $t_a \to 0$, $t_b \to 1$, namely, $(P_{max})_\infty /\mu \approx 2.83945$. Here, the mark ∞ means $b/a \to \infty$. In this paper, however, we are concerned with the case when b/a is finite, so the values t_a, t_b are limited

by (27), and it never happens that $t_a \to 0$, $t_b \to 1$. When a finite ratio b/a is given, P_{max}, the extreme (maximum) value of P, may be obtained by applying Lagrange's method of indeterminate coefficients to (27), (28). We find that P takes its maximum at

$$t_a^2 + t_b^2 + t_a t_b = 1. \tag{31}$$

The relation between b/a and P_{max} is shown in Fig. 1. Moreover, we may prove that when b/a and P (p_{max}) are given, there exist two sets of solution (t_a, t_b) which satisfy (18), (27), (28). (The detailed proof is safely omitted.) We find, therefore, that the axisymmetric solutions are not unique for the boundary conditions subjected to an internal pressure smaller than P_{max}. Also, there exists no solution if the internal pressure is larger than P_{max}.
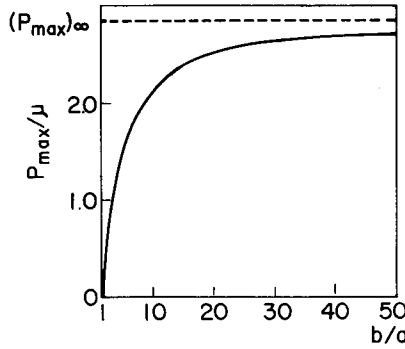

Fig. 1   The relation between the ratio b/a and P_{max}

4.2. Deformation and stress fields

Suppose that R_a and R_b denote the deformed inner and outer radius of a hollow sphere, eqns (16), (19), (25), (26) yield

$$R_a = a t_a^{-3/5} (1 + P/\mu)^{-1/5} \tag{32}$$
$$R_b = b t_b^{-3/5} \tag{33}$$

The relation between **P** and the ratio of the undeformed and deformed inner (outer) radius R_a/a (R_b/b) is displayed in Fig. 2 (Fig. 3) for $a/b = 2, 4, 6$. In both cases, in the beginning, P increases with the deformation and it takes the maximum value P_{max} for a certain deformation, and then decreases after that.
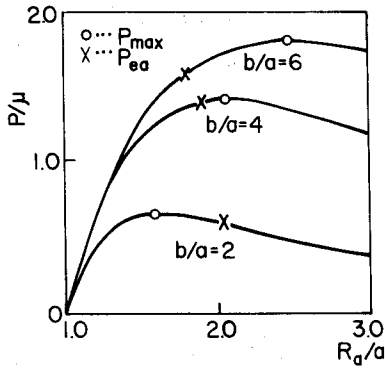
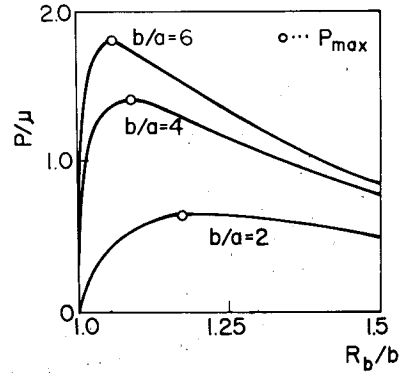Fig. 2 The relation between R_a/a and P Fig. 3 The relation between R_b/b and P

This means that a hollow sphere subjected to an internal pressure indicates an instability phenomenon, if the pressure is given by the load–controlled machine (hard machine). The values of P_{max} are marked with $\bigcirc$ in Figures 2 and 3.

It is also interesting to note that the above result agrees well with the simple experience that when we inflate a balloon, firstly we have to make the pressure larger and larger, and after some level of deformation the balloon is inflated easily with a smaller pressure.

So long as $t < 0$, (4) is always satisfied by (11), so a hollow sphere never collapses (i. e. $R_a < R_b$) for a given pressure. Also, we note from (27), (28), (32), (33) that under the finite ratio of b/a, the deformed radius R_a $(<R_b)$ $\rightarrow \infty$ occurs as t_b $(>t_a)$ $\rightarrow 0$ even with $P \rightarrow 0$.

The resulting stress fields are given by (21), (22), (26)

$$T_r = \mu \left\{ 1 - \sqrt{\frac{h(t_b)(2t_b^2 + 2t_b + 5)^3}{h(t)(2t^2 + 2t + 5)^3}} \right\} \tag{34}$$

$$T_\theta = T_\phi = \mu \left\{ 1 - \sqrt{\frac{h(t_b)(2t_b^2 + 2t_b + 5)^3}{h(t)(2t^2 + 2t + 5)^3 t^{-4}}} \right\} \tag{35}$$

for $t_a < t < t_b$. Because of the mototonical increasing character of H_1 (t), T_R increases monotonically with t (also with r). T_R is always compressive, and the largest value of $|T_R|$ occurs at the inner surface. The distribution of $|T_R|$ for $b/a = 2$ is shown in Fig. 4, where it is to be noted that there are two distributions of $|T_R|$ at a certain value of P. The solid lines indicate the distribution in the case of increasing pressure and the dotted lines indicate those of decreasing pressure.
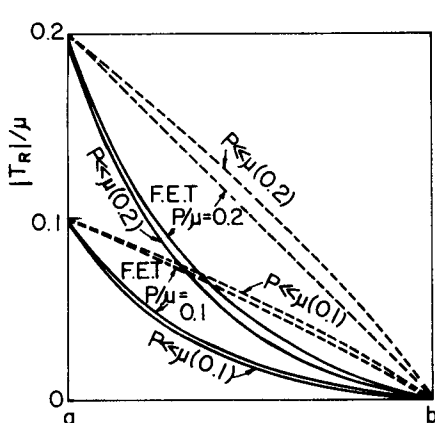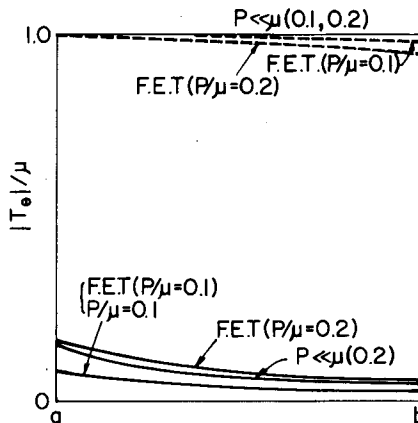
Fig. 4   The distribution of $|T_R|$ $(b/a=2)$

Fig. 5   The distribution of T_θ $(b/a=2)$

To examine the character of T_θ (T_ϕ), we consider the auxiliary function

$$G(t)=h(t)(2t^2+2t+2)^3 t^{-4} \quad for \ 0\le t\le 1. \tag{36}$$

Since $G(t)$ is a monotone decreasing function, T_θ (T_ϕ) decreases monotonically with increasing r. T_θ (T_ϕ) is always tensile and reaches its maximum at the inner surface. The distribution of T_θ for $b/a=2$ is shown in Fig. 5.

Now, the limiting case $P\ll\mu$ is of interest. It is found from (27), (28) that this case appears at $t_a\approx 1$, $t_b\approx 1$, or $t_a\approx 0$ or $t_b\approx 0$, so that $t\approx 1$ or $t\approx 0$ throughout the body. Linearizing eqns (13), (19), (20), (34), and (35) (expanding linearly with respect to t, t_a, t_b), the former case corresponds to the well-known result of the infinitesimal theory of elasticity,

$$T_R=-\frac{Pa^3}{b^3-a^3}\left\{\frac{b^3}{r^3}-1\right\}$$

$$T_\theta=T_\phi=\frac{Pa^3}{b^3-a^3}\left\{\frac{b^3}{2r^3}+1\right\}.$$

The latter case yields

$$T_R\approx -P\frac{b^{5/3}-r^{5/3}}{b^{5/3}-a^{5/3}}$$

$$T_\theta=T_\phi\approx\mu.$$

The linearized distribution of T_θ (T_ϕ) is shown with $P\ll\mu$ in Figures 4 and 5. The former case is drawn with solid lines and the latter one is drawn with

dotted lines. (In **Fig. 5**, the lines of $T_\theta \fallingdotseq \mu$ are above the frame.) As P gets smaller, the results of the above limiting case become closer to the results of the finite elastic theory.

4.3. Loss of ellipticity

As stated above, Blatz–Ko material has a character whereby the governing partial differential equations of equilibrium lose ellipticity at sufficient strain level. Since there may possibly arise *non-smooth* deformation fields in such cases, it may be important to examine when the ellipticity is lost.
Necessary and sufficient conditions for the ellipticity of Blatz–Ko material are very simple, i.e.[3]

$$2-\sqrt{3}<t<2+\sqrt{3}\,. \tag{37}$$

Since we have $t<1$, ellipticity will be lost when the left hand inequality is violated. A hollow sphere loses ellipticity at $r=a$ firstly under the inner pressure P_{ea}. After that, with the pressure increasing, the non–elliptic region spreads gradually, and lastly the non–elliptic region reaches $r=b$ under the pressure P_{eb}. The relations between P_{ea}, P_{eb}, and b/a are shown in **Fig. 6**. Note that P_{eb} is always smaller than P_{ea}. We have $(P_{ea})_\infty \fallingdotseq 0.172582\,\mu$ and $(P_{eb})_\infty \fallingdotseq 0.408549\,\mu$ as $b/a \to \infty$. The values of P_{ea} are marked with $\times$ in **Fig. 2**.
In **Fig. 2**, when b/a is small (approximately when b/a is less than 3.24104), P_{ea} occurs after P_{max}. Substituting $t_b = 2 - \sqrt{3}$ into (33), we find that P_{eb} always occurs after P_{max} at a constant value of $P_b/b \fallingdotseq 2.20378$.
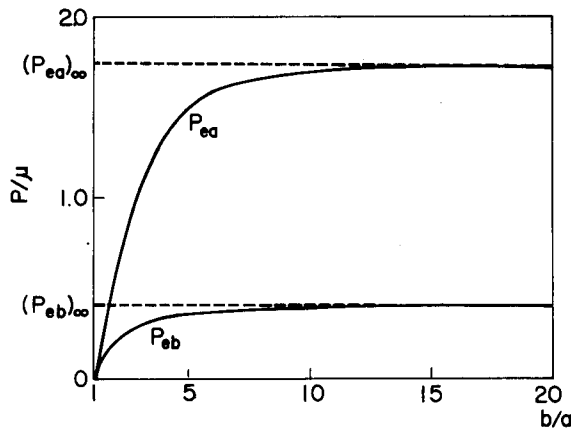

Fig. 6 The relation between the ratio b/a and P_{ea}, P_{eb}

5. The case of external pressure

5.1. Solution to the boundary condtions

The solution method developed in Chapter 3 can also be applied to the case of external pressure. The parameter t is in this case

$$\frac{dt}{dr} < 0, \quad t > 1. \tag{38}$$

(Here, again, detailed proof is omitted.) The boundary conditions are given by

$$T_R = 0 \quad at \ r = a \tag{39}$$
$$T_r = -P \quad at \ r = b. \tag{40}$$

Using (19), (20), (39), and (40), at this time, simultanuous equations (27), (28) are replaced by

$$\frac{a^{15}(1-t_a)^5(2t_a^2+2t_a+5)^2}{t_a^9 h(t_a)} = \frac{b^{15}(1-t_b)^5(2t_b^2+2t_b+5)^2}{t_b^9 h(t_b)} \tag{41}$$

$$h(t_a)(2t_a^2+2t_a+5)^3 = h(t_b)(2t_b^2+2t_b+5)^3(1+P/\mu)^2, \tag{42}$$

where from (38)

$$(1<) < t_b < t < t_a. \tag{43}$$

When the ratio b/a and an external pressure P are given, one may solve these equations and find a unique solution (t_a, t_b) satisfying (43) unlike the internal pressure case. In this case, P_{max} does not exist and so external pressure can be applied arbitrarily.

5.2. Deformation and stress fields

The deformed inner and outer radius R_a, R_b are given by

$$R_a = at_a^{-3/5} \tag{44}$$
$$R_b = bt_b^{-3/5}(1+P/\mu)^{-1/5} \tag{45}$$

Since $t > 0$, a hollow sphere does not collapse for an arbitrary external pressure (i.e. $R_b > R_a$). We note, however, from (30) that $H_2(t) \to 4e^{-x}$ as $t \to \infty$, so for a

given finite b/a, t_b takes a particular finite limit even if $t_a \rightarrow \infty$, which means $P \rightarrow \infty$ by (42) and R_b $(>R_a)$ $\rightarrow 0$ by (44), (45).
the Cauchy stress field is found to be

$$T_R = \mu \left\{ 1 - \sqrt{\frac{h(t_a)(2t_a^2 + 2t_a + 5)^3}{h(t)(2t^2 + 2t + 5)^3}} \right\} \tag{46}$$

$$T_\theta = T_\phi = \mu \left\{ 1 - \sqrt{\frac{h(t_a)(2t_a^2 + 2t_a + 5)^3}{h(t)(2t^2 + 2t + 5)^3 t^{-4}}} \right\}. \tag{47}$$

From (46), one finds that T_R is monotonically decreasing with r since $\dot{H}_1$ (t) > 0 for $t > 1$. T_R is always compressive and the maximum value of $|T_R|$ occurs at the outer surface of a hollow sphere. The distribution of $|T_R|$ throughout the body is shown in Fig. 7.

On the other hand, the behavior of T_θ (T_ϕ) given by (47) is more complicated than that of T_R. It turns out that T_θ is always compressive, but the maximum value of $|T_\theta|_{max}$ does not always occur at the inner surface. The variation of $|T_\theta|$ depends on the sign of $\dot{G}$ (t). Here, we introduce t_m such as $\dot{G}$ $(t_m) = 0$, i. e. $t_m = (\sqrt{21} - 1)/2$. Three cases are to be examoned owing to t_a t_b t_m

(i)   When $t_b < t_a \leq t_m$ G (t) is monotone increasing, so $|T_\theta|$ monotonical decreasing with r. $|T_\theta|_{max}$ occurs at the inner surface.

(ii)   When $t_b < t_m < t_a$ the sign of $\dot{G}$ (t) varies at $t = t_m$ so T_θ takes its minimum at $t = t_m$. $|T_\theta|_{max}$ occurs within the body of a hollow sphere.

(iii)   When $t_b \leq t_a < t_m$ $|T_\theta|$ is monotone increasing with r, and $|T_\theta|_{max}$ appears at the outer surface.
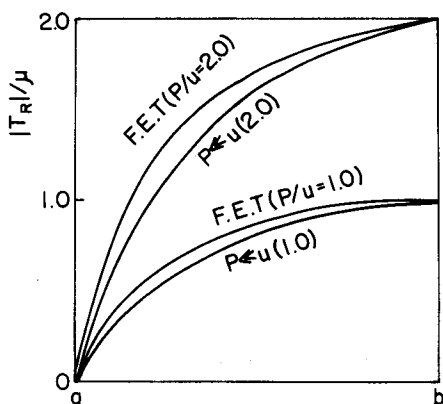

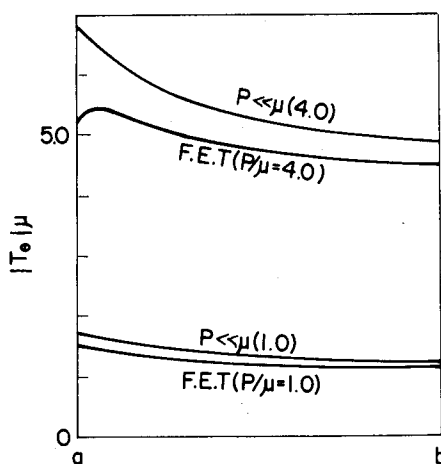Fig. 7   The distribution of $|T_R|$ $(b/a = 2)$

Fig. 8   The distribution of T_θ $(b/a = 2)$

The distribution of $|T_\theta|$ for $b/a = 2$ is shown in Fig. 8. As the pressure gets larger, the location of $|T_\theta|_{max}$ moves into the body (case (ii)). However, the appearance of case (iii) is restricted by the ratio b/a. $|T_\theta|_{max}$ never appeara at the outer surface even though $P \to \infty$, if b/a is larger than the supreme ratio K_m ≈ 1.0853, which is given by substituting $t_b = t_m$ and $t_a \to \infty$ into (41). The supreme location of $|T_\theta|_{max}$ is also $sup \ (r_m/a) \approx 1.0853$.

The relations between b/a and P_a (i.e. the pressure when $|T_\theta|_{max}$ departs from inner surface), P_b (i.e. The pressure when $|T_\theta|_{max}$ appears at the outer surface firstly) are shown in Figures 9 and 10. In Fig. 9, $(P_a)_\infty \approx 1.64322$ as $b/a \to \infty$.

Here, we again consider the case when the applied pressure is sufficiently smoll ($P \ll \mu$). Eqns (41), (42) show that $t_a \approx 1, t_b \approx 1$, so $t \approx 1$ throughout the body. The linearization yields the corresponding infinitesimal elasticity results

$$T_R = \frac{Pb^3}{b^3 - a^3} \left\{ \frac{a^3}{r^3} - 1 \right\}$$

$$T_\theta = T_\phi = -\frac{Pb^3}{b^3 - a^3} \left\{ \frac{a^3}{2r^3} + 1 \right\}.$$

The distribution of linearized T_R, T_θ are shown in Figures 7 and 8 added with $P \ll \mu$.

5.3. Loss of ellipticity

In the present case, since $t > 1$, ellipticity is lost when the right hand inequality of (37) is violated. A hollow sphere loses ellipticity at an inner surface firstly because of (43). Since $t_m \approx 1.79 < t_e \approx 3.73$, $|T_\theta|_{max}$ has already moved into the body before a non-elliptic region appears at the inner surface.
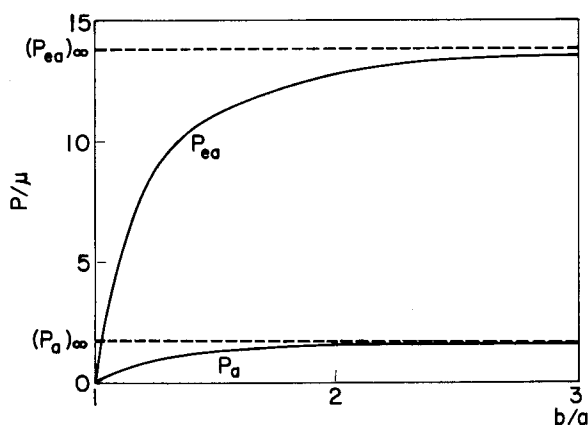

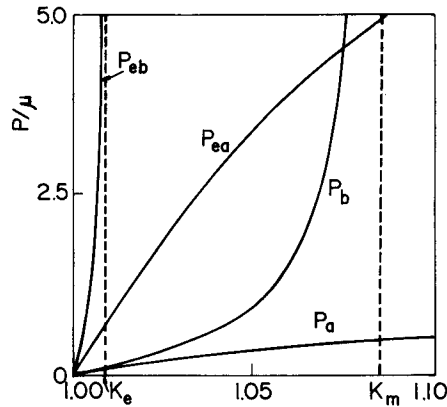Fig. 9   The relation between the ratir b/a and P_a, P_{ea}

Fig. 10   The relation between the ratio b/a and P_a, P_b, P_{ea}, P_{eb}

The relations between P_{ea} (i. e. the pressure when the hollow sphere loses the ellipticity at $r=a$ firstly), and P_{eb} (i. e. the pressure when the non–elliptic region reaches $r=b$) are shown in Figures 9 and 10. As the pressure gets larger, the non–elliptic region spreads. However, whether that region spreads out throughout the body depends on the ratio b/a. The non–elliptic region does not spread out throughout the body if b/a is larger than the supreme ratio $K_e \approx 1.00929$, which is obtained by substituting $t_b=t_e$ and $t_a \to \infty$ into (41). In Fig. 9, $(P_{ea})_\infty \approx 13.7941$.

For example, when the ratio $b/a= 1.03$, after the location $|T_\theta|_{max}$ moves to the outer surface, a non–elliptic region develops from the inner surface, but the region has a limit even if $P \to \infty$. The distribution of $|T_\theta|$ for $b/a= 1.03$ is shown in Fig. 10. In this figure, the non–elliptic region spreads to the mark ◯, and the line without the mark ◯ shows that the region has not appeared yet.

References

1)   P. J. Blatz and W. L. Ko ; Trans. Soc. Rheol., **6**, 223 (1962).

2)   J. K. Knowles and E. J. Sternberg ; J. Elasticity, **5**, 341 (1975).

3)   R. Abeyaratne and C. O. Horgan ; J. Elasticity, **15**, 243 (1985).